Journal of the Serbian Chemical Society
JSCS-info@shd.org.rs • www.shd.org.rs/JSCS
J. Serb. Chem. Soc. 77 (3) 335–348 (2012)
JSCS–4272
UDC 547.979.733–034+543.428.3/.4:
535.375+535.372
Original scientific paper

Synthesis and properties of 5,10,15,20-tetrakis[4-(3,5-dioctyloxybenzamido)phenyl]porphyrin and its metal complexes

WENHUI LIAN, YUANYUAN SUN, BINBIN WANG, NING SHAN and TONGSHUN SHI*

College of Chemistry, Jilin University, Changchun 130023, P. R. China

(Received 16 May, revised 3 October 2011)

Abstract: A novel 5,10,15,20-tetrakis[4-(3,5-dioctyloxybenzamido)phenyl]-porphyrin and its transition metal complexes are reported in this paper. Their molecular structures were characterized by elemental analysis as well as IR, ^{1}H-NMR and UV–Vis spectroscopy. Their spectroscopic properties were studied by Raman and fluorescence spectroscopy, and X-ray photoelectron spectroscopy (XPS). The fluorescence quantum yields were measured at room temperature. The fluorescence intensity of the porphyrin ligand was stronger than the intensity of the complexes. There were large differences in the Raman spectrum of the porphyrin ligand and those of the metal complexes due to changes in the symmetry of porphyrin plane. In the XPS spectra, the replacement of the free-base protons by a metal ion to form the metalloporphyrin not only increases the symmetry of the molecule, but also introduces an electron withdrawing group into the center of the porphyrin ligand, which increases the N_{1s} binding energy.

Keywords: porphyrin; transition metal complex; XPS spectra; Raman spectra; fluorescence spectra.

INTRODUCTION

Recently, investigation of porphyrins has become of increasing interest.[1,2] Porphyrins and metalloporphyrins are functional molecules that are used for a variety of applications and devices, such as optoelectronic, luminescent and, molecular logic devices, supramolecular self-assembly, solar energy harvesting systems, photonic materials, and therapeutics.[3–7]. These applications are affected by the diverse electrochemical and photophysical properties of the porphyrins and the ability to fine-tune these properties by the exocyclic substituents on the macrocycle and *via* the choice of chelated metal ion.

Porphyrins have many desirable features, such as high stability, intense absorption of sunlight, a highly conjugated plane and a small gap between the high-

* Corresponding author. E-mail: wenhuilian1984@hotmail.com
doi: 10.2298/JSC110516190L

est occupied molecular orbital (HOMO) and lowest unoccupied molecular orbital (LUMO) energy level. The highly conjugated π-electron skeleton of a porphyrin provides an adequate number of π electrons and π–π* transitions normally give a strong absorption in the UV and visible regions of the spectrum.[8] Metalloporphyrins generally have high thermal stability and show strong electronic transitions in the visible and ultraviolet regions. In order to evaluate the applications of metalloporphyrins, it is necessary to understand the electronic structure and photophysical properties. Raman spectroscopy, fluorescence spectra, X-ray photoelectron spectroscopy, *etc*, have been widely used to study the porphyrin ligand and metalloporphyrins, and the results could provide important information to determine their electronic structure. X-Ray photoelectron spectroscopy (XPS) is a powerful tool for the characterization of both the chemical composition and the electronic environments of each atom in a molecular system.[9–11]

To date, the synthesis and application of the substituent tetraphenylporphyrin (TPP) bearing special functional groups have caused great interest, but those bearing an amide group as side chains have been little reported. In this research, a novel TPP derivative bearing an amide group and its transition metal complexes were synthesized. The benzene core was replaced by a rigid porphyrin core, which is linked *via* amide bonds to four triphenylenes. Since the porphyrin dimension is much larger than that of a benzene ring and the symmetry changes from three-fold to four-fold, an entirely different self-assembly *via* hydrogen bonding was to be expected. Their structures were characterized by their UV–Vis, IR and ^{1}H-NMR spectra and the changes in the fluorescence, Raman spectra and XPS behavior of these compounds were investigated.

RESULTS AND DISCUSSION

*Physical, analytic and spectral data for **7a**–**7d***

*5,10,15,20-Tetrakis[4-(3,5-dioctyloxybenzamido)phenyl]porphyrin (**7a**)*. Purple solid. Yield: 62.4 %; Anal. Calcd. for $C_{136}H_{178}N_8O_{12}$: C, 77.12; H, 8.42; N, 5.26 %. Found: C, 77.16; H, 8.48; N, 5.20 %. IR (KBr, cm^{-1}): 3314 (N–H, pyrrole), 2925, 2855 (C–H), 1674 (C=O), 1523 (N–H, amide), 1245 (Ar–O–C), 966 (N–H, pyrrole), 721 (–$(CH_2)_n$–, $n > 4$). ^{1}H-NMR (500MHz, $CDCl_3$, δ / ppm): 8.92 (8H, *s*, pyrrole ring), 8.30 (4H, *s*, –NH–CO–), 8.20–8.26 (8H, *d*, J = 30 Hz, *o*–C_6H_4), 8.08–8.03 (8H, *d*, J = 25 Hz, *m*-C_6H_4), 6.98–7.04 (8H, *d*, J = 30 Hz, *o*–C_6H_3), 6.64–6.69 (4H, *d*, J = 25 Hz, *m*–C_6H_3), 4.10–4.22 (16H, *m*, –O–CH_2–), 1.78–1.98 (16H, *m*, –O–C–CH_2–), 1.49–1.64(16H, *m*, –CH_2–CH_3), 1.21–1.40 (64H, *m*, –O–C–C–$(CH_2)_4$–C–CH_3), 0.85–0.95 (24H, *t*, J = 25 Hz, –O–C–C–$(C)_4$–C–CH_3), –2.74 (2H, *s*, N–H, pyrrole). UV–Vis ($CHCl_3$, λ_{max} / nm): 425 (Soret band), 520, 555, 595, 650 (four Q bands).

*Zinc 5,10,15,20-tetrakis[4-(3,5-dioctyloxybenzamido)phenyl]porphyrin (**7b**)*. Purple red solid. Yield: 90.5 %; Anal. Calcd. for $C_{136}H_{176}N_8O_{12}Zn$: C, 74.93; H,

8.35; N, 5.02 %. Found: C, 74.99; H, 8.30; N, 5.07 %. IR (KBr, cm^{-1}): 3285 (N–H, imide), 2924, 2851 (C–H), 1664 (C=O), 1527 (N–H, amide), 1245 (Ar–O–C), 996 (N–Zn), 721 (–$(CH_2)_n$–, $n > 4$). ^{1}H-NMR (500 MHz ,$CDCl_3$, δ / ppm), 8.99 (8H, *s*, pyrrole ring), 8.12–8.30 (8H, *d*, J = 40 Hz, *o*–C_6H_4), 8.06 (4H, *s*,–CON–H), 7.95–7.96 (8H, *d*, J = 5 Hz, *m*–C_6H_4), 7.26–7.27 (8H, *d*, J = 5 Hz, *o*–C_6H_3), 6.96–6.87 (4H, *t*, J = 22.5 Hz, *m*-C_6H_3), 3.92–4.03 (16H, *t*, J = 7.5 Hz, –O–CH_2–), 1.68–1.98 (16H, *m*, –O–C–CH_2–), 1.22–1.52 (80H, *m*, –C–C–$(CH_2)_5$–CH_3), 0.861–0.905 (24H, *t*, J = 11 Hz, –C–C–$(C)_5$–CH_3). UV–Vis ($CHCl_3$, λ_{max} / nm): 425 (Soret band), 551, 592 (two Q bands).

*Manganese 5,10,15,20-tetrakis[4-(3,5-dioctyloxybenzamido)phenyl]porphyrin (**7c**)*. Dark green solid. Yield: 82.4 %; Anal. Calcd. for $C_{136}H_{176}MnN_8O_{12}Cl$: C, 74.12; H, 7.99; N, 5.04 %. Found: C, 74.07; H, 8.04; N, 5.08 %. IR (KBr, cm^{-1}): 3282 (N–H, imide), 2925, 2854 (C–H), 1677 (C=O), 1519 (N–H, amide), 1244 (Ar–O–C), 1008 (N–Mn), 721 (–$(CH_2)_n$–, $n > 4$). UV–Vis ($CHCl_3$, λ_{max} / nm): 480 (Soret band), 585, 625 (two Q bands).

*Cobalt 5,10,15,20-tetrakis[4-(3,5-dioctyloxybenzamide)phenyl]porphyrin (**7d**)*. Purple red solid. Yield: 85.7 %; Anal. Calcd. for $C_{136}H_{176}CoN_8O_{12}$: C, 75.21; H, 8.11; N, 5.09 %. Found: C, 75.14; H, 8.16 N, 5.15 %. IR (KBr, cm^{-1}) 3280 (N–H (imide)), 2925, 2854 (C–H), 1658 (C=O), 1517 (N–H, amide), 1252 (Ar–O–C), 1000 (N–Co), 717 (–$(CH_2)_n$–, $n > 4$). UV–vis ($CHCl_3$, λ_{max} / nm): 415 (Soret band), 530, 675 (two Q bands).

UV–Vis spectra

The electronic absorption spectra of porphyrins result from electronic transitions from the ground state (S_0) to the two lowest singlet excited states S_1 and S_2. The $S_0 \rightarrow S_1$ transition gives rise to weak Q bands in the visible region while the $S_0 \rightarrow S_2$ transition produces a strong Soret band in the near UV region.[12,13] The absorption bands of **7a** appear at 425, 520, 555, 595 and 650 nm. Compared with the absorption bands of TPP, the absorption bands of **7a** are red-shifted.[14] Possibly, this is because the substituent group on the phenyl group at the meso-position of the porphyrin ring is an electron-donating group, thereby enabling the electronic density on the phenyl ring to strengthen. Thus, the phenyl ring conjugates to a certain degree with the porphyrin macrocycle. This kind of conjugation action causes a reduction of the electron transition energy of the porphyrin macrocycle, resulting in red shifts of the absorption bands.

When a metal atom is bonded to the central nitrogen atoms of a porphyrin, the metal ion accepts the lone-pair-electrons of the N atoms of the pyrrole rings, while the metal ion donates the electrons to the porphyrin molecule, forming delocalized π bonds, which permit the easy flow of electrons within the delocalized π system. In this work, the UV–Vis spectra of the metalloporphyrins exhibited one Soret band and either one or two Q bands; the number of Q band decreases

and the absorption frequencies shift. When the metal ion coordinates with porphyrin ligand, the symmetry of the molecule is changed from D_{2h} to D_{4h}, the cleavage degree of the molecular orbital decreases and the degeneracy increases; hence, the number of Q bands therefore decreases.

Infrared spectra

The IR bands at 3314 and 966 cm^{-1} of **7a** are attributed to N–H stretching and bending vibrations of the porphyrin ligand core, respectively, but they were absent in the spectra of the complexes, because the hydrogen atom in the N–H bond was replaced by a transition metal ion.[15] In addition, a new band in the spectrum of **7b**, **7c** and **7d** appeared at 996, 1008 and 1000 cm^{-1}, respectively, which is characteristic of metalloporphyrins. The bands at about 3280–3285 cm^{-1} of the complexes are assigned to N–H stretching vibrations of the amide group on the side chains, but in the spectrum of the porphyrin ligand, it overlapped the N–H stretching vibration of the porphyrin core and could not be distinguished. The bands in the range of 1652–1670 cm^{-1} are assigned to C=O stretching vibration (amide I). The bands at about 1517–1521 cm^{-1} are assigned to N–H in-plane bending and C–N stretching (imide II). The bands at about 1245–1252cm^{-1} are assigned to Ar–O–C stretching vibrations. The bands at 717–721 cm^{-1} are assigned to the methylene in-plane rocking vibration of a straight alkyl chain containing more than four carbon atoms.

Fluorescence spectra

Excited-state processes in porphyrins are extremely important for their application in molecular devices. The room temperature fluorescence spectra of the porphyrin ligand and metalloporphyrins in chloroform (2×10^{-6} mol L^{-1}) were recorded. No fluorescence signal was detected for the metalloporphyrins **7c** and **7d**

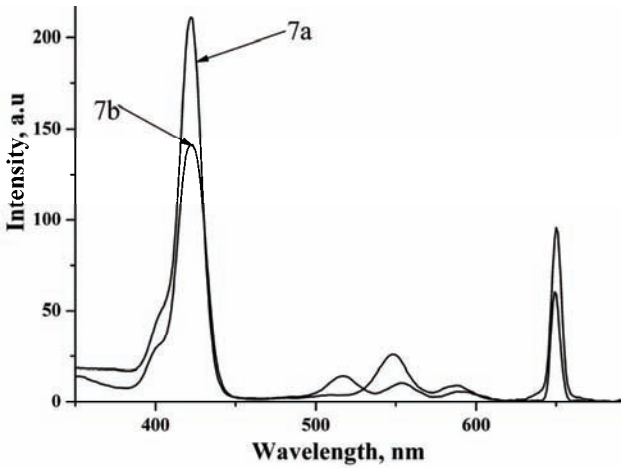

Fig. 1. Excitation spectra of **7a** and **7b** in chloroform.

under the employed experimental conditions. The excitation spectra of **7a** and **7b** are shown in Fig. 1. In the region of 350–700 nm, the excitation spectra are approximately mirror images of the absorption spectra, indicating that they correspond to a similar electron transition process.

The emission spectra of **7a** and **7b** are shown in Fig. 2 for an excitation wavelength of 420 nm. The emission spectra data of **7a** and **7b** are given in Table I. Excitation to the S_2 (B band) and the S_1 (Q band) in porphyrin compounds results in fluorescence. The fluorescence of the S_2 (B band) is attributed to the transition from the second excited singlet state S_2 to the ground state S_0, $S_2 \rightarrow S_0$, and it corresponds with the Soret band in the electronic absorption spectra. In addition, fluorescence of the Q band is attributed to the transition from the lowest excited singlet state S_1 to the ground state S_0. The fluorescence of $S_2 \rightarrow S_0$ was too weak to be observed in this study, owing to light scattering and resorption of strong Soret absorption band. It is well known that metal-free porphyrins usually show two strong emission bands around 650 and 720 nm.[16] The fluorescence bands of **7a** were at 653 and 716 nm. Compared with the fluorescent bands at 650 and 713 nm of TPP, the emission peaks of porphyrin ligand were red-shifted by 3 nm. The fluorescence bands of the Zn complex were at 597 and 644 nm, which were red-shifted compared to ZnTPP (592 and 641 nm). These red shifts may be due to the interaction of the arylamido group with the conjugated π-electron system of the porphyrin macrocycle. The conjugation of the porphyrin macrocycle is affected by the electronic donating groups. The conjugation is enhanced when the alkylamide groups are linked on the phenyl group.

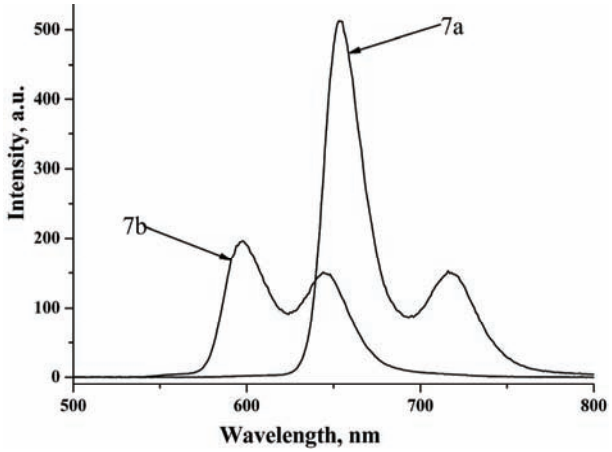

Fig. 2. Fluorescence spectra of **7a** and **7b** in chloroform.

The quantum yield of porphyrin ligand and Zn complex were calculated according to the following equation:

$$\phi_{\text{sample}} = \frac{F_{\text{sample}}}{F_{\text{ZnTPP}}} \frac{A_{\text{ZnTPP}}}{A_{\text{sample}}} \phi_{\text{ZnTPP}}$$

where F_{sample} and F_{ZnTPP} are the measured fluorescence integral areas of the sample and the reference ZnTPP, respectively. A_{sample} and A_{ZnTPP} are the absorbance of the sample and the reference, respectively. ϕ_{sample} and ϕ_{ZnTPP} (ϕ_{ZnTPP} = = 0.033)[17] are the quantum yields of the sample and the reference ZnTPP at same excitation wavelength. The quantum yields of the porphyrin ligand are much lower than that of TPP (ϕ_{TPP} = 0.11[18]). As is known, porphyrins can be considered as specific donor–acceptor systems, and the decrease in the fluorescence quantum yields of the porphyrin ligand in comparison to that of TPP could be the result of intramolecular energy migration or electron transfer from the donor part of the molecule to the acceptor part. The fluorescence quantum yields of **7a** and **7b** were very small. Thus, the excited state S_1 was primarily deactivated by radiationless decay in porphyrins. This indicates fairly certainly that the spin forbidden process $S_1 \rightarrow Tn$ is dominant for the radiationless deactivation of S_1 in porphyrin compounds. The fluorescence yield of **7b** was much smaller than that of **7a** because zinc weakened the fluorescence radiation.

TABLE I. Emission spectra data and quantum yields (ϕ_f) of **7a** and **7b**

Compound	*Q*(0–0) / nm	Q(0–1) / nm	ϕ_f
7a	653	716	0.064
7b	597	644	0.032

Resonance Raman spectra

The resonance Raman spectra of the porphyrin ligand and complexes were obtained by excitation at 514.5 nm. The important Raman frequencies and their assignments are listed in Table II. The Raman spectra of the porphyrin ligand and the Mn complex are shown in Fig. 3. The resonance Raman spectra of tetraphenylporphyrin derivatives have been studied extensively.[19–21] Thus, the assignments of Raman bands of porphyrin ligand and complexes are only discussed briefly here.

TABLE II. Raman spectra and assignment of the porphyrin ligand and its complexes (*vs*: very strong, *s*: strong, *m*: medium, *w*: weak)

Compound				Assigned
7a	**7b**	**7c**	**7d**	
1553*vs*	1550*s*	1573*vs*	1561*vs*	ν_2, $\nu(C_\beta C_\beta)$
1496*m*	1494*m*	1497*s*	1502*m*	ϕ_5, phenyl
1455*s*	1454*w*	1456*m*	1455*w*	ν_3, $\nu(C_\alpha C_m)$
1360*m*	1353*s*	1372*m*	1367*s*	ν_4, $\nu(C_\alpha\text{–}N)$ / $\nu(C_\alpha C_\beta)$
1330*m*	–	1341*w*	–	ν_{20}, ν(pyr. quarter-ring)

1240*m*	1242*w*	1241*m*	1242*w*	ν_1, $\nu(C_m–Ph)$
1081*w*	1067*w*	1086*m*	1076*m*	ν_{17}, $\delta(C_\beta–H)$
1002*m*	1008*m*	1002*m*	997*w*	ν_{15}, ν(pyr. breath.) + phenyl

TABLE II. Continued

Compound				Assigned
7a	**7b**	**7c**	**7d**	
963*w*	–	–	–	ν_6, ν(pyrrole breath.)
719*w*	717*w*	713*w*	710*w*	π_3, phenyl
	404*w*	397*w*	395	ν(M–N)
335	–	313*w*	312*w*	ν_8, ν(pyr. translation)

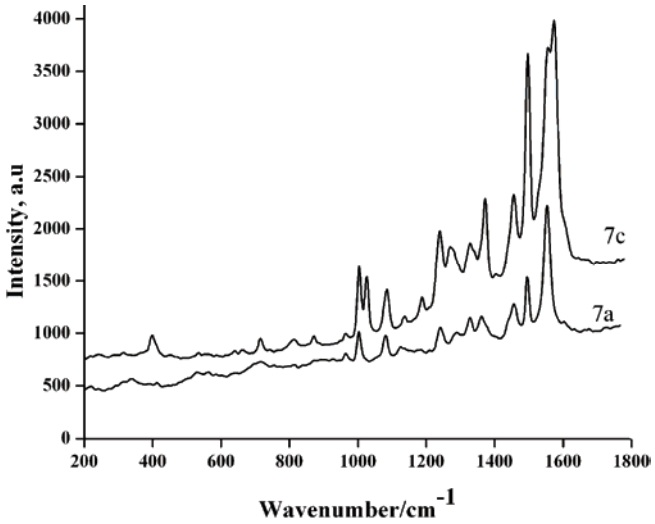

Fig. 3. Raman spectra of the porphyrin ligand and the Mn complex.

In the 900–1650 cm^{-1} high-frequency region of the Raman spectra of porphyrin ligand and complexes, Raman bands generally arise from the totally symmetric vibrational modes, such as $C_\beta C_\beta$, $C_\alpha C_\beta$, $C_\alpha C_m$, pyrrole quarter-ring, and pyrrole half-ring stretching. The wavenumber positions of Raman bands in the high-frequency region are sensitive to the core size, axial ligation and electron density of the central metal ion. In this region, the band at 1553 cm^{-1} of porphyrin ligand was assigned to the $C_\beta C_\beta$ stretch ν_2 mode, which was up-shifted to 1573 cm^{-1} in the Mn complex and to 1561 cm^{-1} in Co complex, but it was down-shifted to 1548 cm^{-1} in the Zn complex. The ν_2 mode was observed with enhanced intensity in the complexes. In fact, it is one of the most intense bands in the high-frequency region. The band at 1496 cm^{-1} of porphyrin ligand was assigned to the vibration of phenyl ring, and it was little shifted in the complexes, which confirmed that the metal ion had little effect on the phenyl at the meso

positions. Raman bands in 1300–1450 cm^{-1} were due to the out-of-phase coupled $C_\alpha C_\beta/C_\alpha N$ stretching modes. The 1360 and 1330 cm^{-1} bands of the porphyrin ligand were assigned to the ν_4 and ν_{20} mode, respectively. The ν_4 mode of **7b**, **7c** and **7d** appeared at 1353, 1372 and 1367 cm^{-1}, respectively. The ν_{20} mode of **7c** shifted to 1341 cm^{-1}, while the ν_{20} mode of **7b** and **7d** were too weak to be observed in the present experiments. The 1240 cm^{-1} band of the porphyrin ligand and the 1240–1242 cm^{-1} band of the complexes were attributed to the Cm−ph stretching ν_1 mode. The band at 1081 cm^{-1} of the porphyrin ligand was assigned to the vibrations of the pyrrole C_β–H stretching ν_9 mode, which shifted to 1067, 1086 and 1076 cm^{-1} in **7b**, **7c** and **7d**, respectively. The band at 1002 cm^{-1} of the porphyrin ligand was assigned to the vibration of pyrrole breathing and phenyl stretching ν_{15} mode, which did not shift in the Mn complex, but was up-shifted to 1008 cm^{-1} in the Zn complex and downshifted to 997 cm^{-1} in the Co complex. The band at 963 cm^{-1} of the porphyrin ligand was assigned to pyrrole breathing ν_6 mode, but it was absent in the spectra of the metalloporphyrins because the hydrogen atom in the N−H bonding had been replaced by a metal ion. In the low--frequency region, the Raman bands of the metalloporphyrin complexes were very different to those of the porphyrin ligand because the structures or vibrational dynamics, especially around the $C_\alpha C_m C_\beta$ bond-angles, were altered by the metal ions. For the porphyrin ligand, the only weak Raman band was observed at 335 cm^{-1}, which was assigned to the ν_8 mode. The ν_8 mode consists of the in--plane translational motion of the pyrrole, which can be described as a uniform breathing of the whole porphine ring accompanied by an in-plane deformation of $C_\alpha C_m C_\beta$ in the pyrrole ring.[22]

X-Ray photoelectron spectra

The XPS spectra of the porphyrin films were obtained. All elements of the porphyrins, including C, N, O and different metals for the metalloporphyrins, were found in the XPS spectra of their films grafted on Si (100). The X-ray photoelectron spectra data of the porphyrin ligand and its complexes are given in Table III. The XPS spectra of the N_{1s} region are shown in Fig. 4.

TABLE III. Binding energies (eV) of the porphyrin ligand and complexes obtained in the XPS experiments

Signal	Compound			
	7a	**7b**	**7c**	**7d**
=N–	397.65	–	–	–
–NH–	399.75	399.60	399.85	399.49
–N–M–	–	397.84	398.65	398.70
C1s	285.03	284.75	284.69	284.60
M2p3/2	–	1021.10	642.40	780.08
O1s	532.9	532.95	532.95	532

Free base porphyrins exhibit two distinct N_{1s} signals corresponding to the imine (–C=N–) nitrogen and the pyrrole (–NH–) nitrogen. The pyrrole nitrogen usually has a higher N_{1s} binding energy than the imine nitrogen.[23–26] The N_{1s} binding energies of these species were ≈400 and ≈397 eV, respectively, so that they should have been readily resolved in the performed experiment. In the porphyrin ligand **7a**, two N signals could be observed, one related to the N atoms of unprotonated porphyrin rings (397.65 eV), and the other to the N atoms of protonated porphyrin-rings and the N atoms of the amide around the porphyrin-ring (399.75 eV). The N_{1s} spectra of the metalloporphyrins also exhibited two signals, the signal with the lower binding energy can be assigned to the metal-binding nitrogen atoms. The binding energy of the protonated porphyrin-ring nitrogen coincides with the amide nitrogen, and their band energies were higher than for the unprotonated porphyrin-ring. This is because of the protonation of the imine nitrogen atoms, which decreases the intensity of the N_{1s} peak at the lower binding energy.

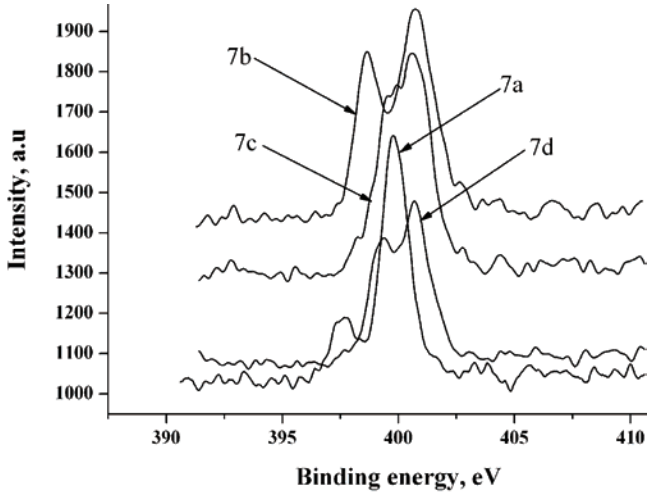

Fig. 4. N_{1s} region of the porphyrin ligand and its complexes.

The metal ion region of the XPS spectra of the films of metalloporphyrins **7b**, **7c**, and **7d** on the Si (100) surface are shown in Fig. 4. The metalloporphryins exhibit a $2p_{3/2}$ signal. The $M2p_{3/2}$ (M = Zn, Mn or Co) region of **7b**, **7c** and **7d** shows sharp peaks with bonding energy at 1021.10, 642.40 and 780.08 eV, respectively, and it is lower than the $M2p_{3/2}$ binding energy of corresponding metal salt. This indicates that the metal atoms accept electrons from the porphyrin ring when they generate complexes. The electrons of the porphyrin-ring nitrogens transfer to an unoccupied metal orbital, *i.e.*, they formed electron donor–acceptor complexes.

EXPERIMENTAL

General synthesis procedures

Chemicals and solvents were obtained from various commercial sources and used without further purification unless otherwise stated. Pyrrole was freshly distilled before use. DMF was pre-dried over activated 4Å molecular sieve and vacuum distilled from calcium hydride (CaH_2) prior to use. Dry $CHCl_3$ and Et_3N were obtained by redistillation from CaH_2. Acetone was dried with anhydrous magnesium sulfate. Anhydrous potassium carbonate was dried under vacuum at 80 °C for 30 min.

The synthesis procedures are illustrated in Schemes 1 and 2. 5,10,15,20-Tetra-(4-nitrophenyl)porphyrin was synthesized through the reaction between pyrrole and *p*-nitrobenzaldehyde in the presence of lactic acid according to a published procedure.[27] 5,10,15,20-Tetra(4-aminophenyl)porphyrin ($TAPPH_2$) was prepared using $SnCl_2$/HCl according to the method of Kruper.[28]

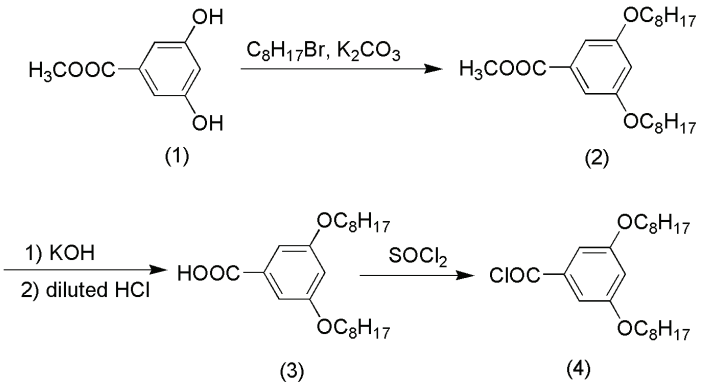

Scheme 1. Synthetic route to 3,5-dioctyloxybenzoyl chloride.

*Methyl 3,5-dioctyloxybenzoate (**2**)*. Compound **1** (3.36 g, 20.0 mmol), anhydrous potassium carbonate (8.28 g, 60.0 mmol) and a catalytic amount of KI in acetone (150 ml) were refluxed for 0.5 h and then 1-bromooctane (9.6 g, 50 mmol) was added in the solution. The reaction mixture was gently refluxed for 36 h under an N_2 atmosphere. The resulting mixture was filtered to remove the impurities. The solution was evaporated to dryness. The solid remaining was recrystallized from methanol to obtain **2** (m.p. 32 °C; yield: 89 %).

*3,5-Dioctyloxybenzoic acid (**3**)*. It was synthesized according to a method similar to that described in previous papers.[29,30] The product was recrystallized from ethanol (m.p. 53 °C; yield: 92 %).

*3,5-Dioctyloxybenzoyl chloride (**4**)*. Compound **3** (3.78 g, 10.0 mmol) was dissolved in 20 ml thionyl chloride. The solution was refluxed for 12 h and then the solvent was evaporated using a water vacuum pump.

*Synthesis of the ligand 5,10,15,20-tetrakis[4-(3,5-dioctyloxybenzamido)phenyl]porphyrin (**7a**)*

A mixture of $TAPPH_2$ (1.2 g, 1.8 mmol) and 3,5-dioctoxybenzoyl chloride (3.96 g, 10.0 mmol) was dissolved in 150 ml freshly distilled $CHCl_3$ and then 3 ml triethylamine was added into the system. The mixture was stirred at room temperature for 2 h, then refluxed for 10 h and cooled to room temperature. The resulting mixture was poured into 150 ml distilled water,

extracted four times with freshly distilled chloroform and then dried over anhydrous magnesium sulfate. The solvent was removed on a rotary evaporator. The residue was further purified by column chromatography (silica gel); the eluent was chloroform followed by chloroform/ethanol=50:1 (v:v). The first band was collected and evaporated to dryness to give a purple solid, which was further recrystallized from chloroform/methanol.

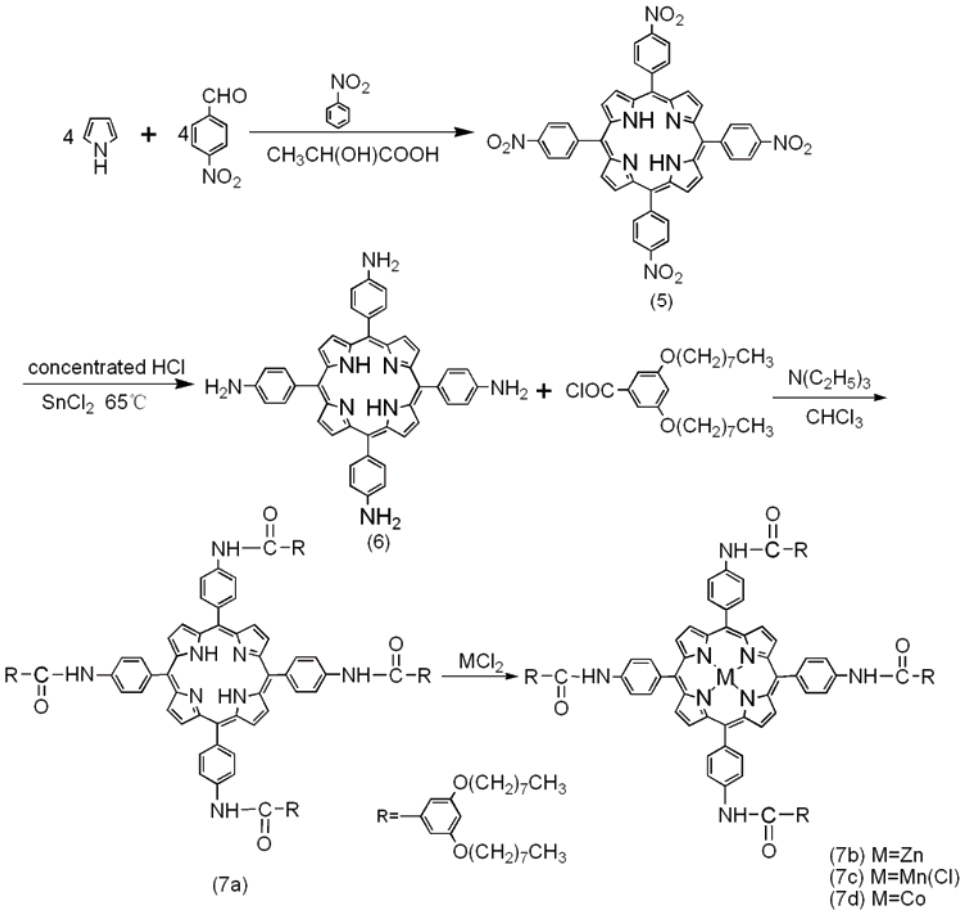

Scheme 2. Synthetic route to the porphyrin ligand and its metal complexes.

*Synthesis of zinc 5,10,15,20-tetrakis[4-(3,5-dioctyloxybenzamido)phenyl]porphyrin (**7b**)*

Compound **7a** (80 mg) and $ZnCl_2$ (100 mg) were dispersed in a mixture of $CHCl_3$ and methanol (2:1). The reaction mixture was refluxed for about 1.5 h. The progress of the reaction was monitored by measuring the UV–Vis spectrum of the reaction solution. The resulting mixture was washed with saturated aqueous NaCl solution and then concentrated. The product was purified by column chromatography on silica gel; eluent: $CHCl_3/C_2H_5OH$, 10:1 (v:v). The second band was collected, dried under vacuum to give a purple red solid.

*Synthesis of manganese 5,10,15,20-tetrakis[4-(3,5-dioctyloxybenzamido)phenyl]porphyrin (**7c**)*

Complex **7c** was prepared by reaction of **7a** (100 mg) with $MnCl_2 \cdot 4H_2O$ (120 mg) in a mixture of freshly distilled $CHCl_3$ (10 ml) and dried DMF (15 ml) at 70 °C under an N_2 atmosphere for about 4 h. The progress of the reaction was also monitored by measuring the UV–Visible spectrum of the reaction mixture. After completion of the reaction, the resulting mixture was cooled, extracted several times with $CHCl_3$ and distilled water. Then the solvent was removed to dryness, and the product was chromatographed on a silica gel column using the eluent $CHCl_3/C_2H_5OH$ 10:1 (v:v).

*Synthesis of cobalt 5,10,15,20-tetrakis[4-(3,5-dioctyloxybenzamido)phenyl]porphyrin (**7d**)*

Compound **7d** was synthesized in a similar manner to that described for **7c**.

Characterization

The ^{1}H-NMR spectra were acquired on a Varian Unity-500 (MHz) NMR spectrometer using standard pulse sequences. The spectra were recorded at 298 K in $CDCl_3$, unless otherwise stated. Chemical shifts are reported on the δ scale relative to TMS. Elemental analyses were performed on a Perkin-Elmer 240 C auto elementary analyzer. The infrared spectra were obtained using a Nicolet 5PC-FT-IR spectrometer in the region of 4000–400 cm^{-1}. The electronic absorption spectra were measured with a Shimadzu UV-3000 spectrometer. Steady-state emission measurements were obtained on a Shimadzu RF-5301PC fluorescence spectrometer with both the excitation and emission slit set at 5 nm. The resonance Raman (RR) spectra were obtained using a Renishaw inVia microscopic instrument. Radiation of 514.5 nm was obtained from an Ar^+ laser. The chemical composition of the surface was investigated by X-ray photoelectron spectroscopy using an ESCALAB Mark II spectrometer.

CONCLUSIONS

In this study, a novel *meso*-tetrakis[4-(3,5-dioctyloxybenzamido)phenyl]porphyrin and its transition metal complexes were synthesized and characterized. Their properties were clearly influenced by the nature of the central transition metal ions. Compared with the porphyrin ligand, the number of the electronic absorption bands of the complexes decreased and exhibited some shifts. The fluorescence results showed that the transition metal in the central porphyrin ring quenched the fluorescence of porphyrin. From the XPS spectra, the information concerning the character of the chemical bonding in the porphyrin ligand and its complexes was obtained. In addition, the investigation could provide very useful information for further study of these derivatives.

Acknowledgement. This work was supported by the National Natural Science Foundation of the People's Republic of China.

ИЗВОД

СИНТЕЗА И СВОЈСТВА 5,10,15,20-ТЕТРАКИС[4-(3,5-ДИОКТИЛОКСИБЕНЗАМИДО)-ФЕНИЛ]ПОРФИРИНА И ЊЕГОВИХ МЕТАЛНИХ КОМПЛЕКСА

WENHUI LIAN, YUANYUAN SUN, BINBIN WANG, NING SHAN и TONGSHUN SHI

College of Chemistry, Jilin University, Changchun 130023, P. R. China

Приказан је нови 5,10,15,20-тетракис[4-(3,5-диоктилоксибензамидо)фенил]порфирин и његови комплекси са прелазним металима. Молекулске структуре окарактерисане су елемен-

талном анализом као и IR, ^{1}H-NMR и UV–Vis спектрима. Спектроскопска својства проучавана су раманском, флуоресцентном и фотоелектронском спектроскопијом X-зрачења (XPS). Квантни флуоресцентни приноси одређивани су на собној температури. Нађено је да је интензитет флуоресценције за порфирински лиганд већи него за комплекс. Уочена је и већа разлика између раманских спектара порфиринског лиганда и његових комплекса, што потиче од симетрије порфиринске равни. Из XPS спектара произилази да замена протона металним јоном у формирању метал-порфирина повећава молекулску симетрију и уводи у центар порфирина електрон-привлачну групу, што повећава N_{1s} енергију везивања.

(Примљено 16. маја, ревидирано 3. октобра 2011)

REFERENCES

1. G. A. Bogdanovic, V. Medakovic, M. K. Milcic, S. D. Zaric, *Int. J. Mol. Sci.* **5** (2004) 174
2. P. I. Premović, I. R. Tonsa, D. M. Đorđević, M. S. Pavlović, *J. Serb. Chem. Soc.* **65** (2000) 113
3. R. K. Lammi, A. Ambroise, T. Balasubramanian, R. W. Wagner, D. F. Bocian, D. Holten, J. S. Lindsey, *J. Am. Chem. Soc.* **122** (2000) 7579
4. C. M. Drain, X. Chen, *Encyclopedia of Nanoscience & Nanotechnology*, American Scientific Press, New York, 2004, pp. 593–616
5. F. Remacle, S. Speiser, R. D. Levine, *J. Phys. Chem., B* **105** (2001) 5589
6. P. Bhyrappa, G. Vaijayanthimala, B. Verghese, *Tetrahedron Lett.* **43** (2002) 6427
7. C. M. Drain, I. Goldberg, I. Sylvain, A. Falber, *Top. Curr. Chem.* **245** (2005) 55
8. R. H. Jin, *Chem. Commun.* (2002) 198
9. D. M. Chen, T. J. He, D.-F. Cong, Y.-H. Zhang, F.-C. Liu, *J. Phys. Chem., A* **105** (2001) 3981
10. C. Y. Lin, T. G. Spiro, *Inorg. Chem*. **35** (1996) 5237
11. A. Rienzo, L. C. Mayor, G. Magnano, C. J. Satterley, E. Ataman, *J. Chem. Phys.* **132** (2010) 084703
12. M. H. Qi, G. F. Liu, *Solid State Sci.* **6** (2004) 287
13. D. M. Chen, Y. H. Zhang, T. J. He, F. C. Liu, *Spectrochim. Acta, A* **58** (2002) 2291
14. M. B. Lan, H. L. Zhao, H. H. Yuan, C. R. Jiang, S. H. Zou, Y. Jiang, *Dyes Pigm.* **74** (2007) 357
15. W. Liu, Y. H. Shi, T. S. Shi, *Chem. J. Chin. Univ.* **24** (2003) 200
16. X. Zhang, Y. Li, D. Qi, J. Jiang, X. Yan, Y. Bian, *J. Phys. Chem., B* **114** (2010) 13143
17. S. S. Song, D. M. Li, J. F. Wu, C. F. Zhuang, H, Ding, *Eur. J. Inorg. Chem.* (2007) 1844
18. B. D. Stasio, C. Frochot, D. Dumas, P. Even, J. Zwier, F. Guillemin, M. L. Viriot, M. Barberi-Heyob, *Eur. J. Med. Chem.* **40** (2005) 1111
19. G. S. S. Saini, *Spectrochim. Acta, A* **64** (2006) 981
20. F. Paulat, V. K. K. Praneeth, C. Nather, N. Lehnert, *Inorg. Chem.* **45** (2006) 2835
21. I. Halvorsen., E. Steene., A. Ghosh, *J. Porphyrins Phthalocyanines* **5** (2001) 721
22. P. M. Kozlowski, A. A. Jarzecki, P. Pulay, X. Y. Li, M. Z. Zgierski, *J. Phys. Chem.* **100** (1996) 13885
23. J. M. Gottfried, K. Flechtner, A. Kretschmann, T. Lukasczyk, H. P. Steinruck, *J. Am. Chem. Soc.* **128** (2006) 5644
24. N. Nishimura, M. Ooi, K. Shimazu, H. Fujii, K. Uosaki, *J. Electroanal. Chem.* **473** (1999) 75
25. D. K. Sarkar, X. J. Zhou, A. Tannous, M. Louis, K. T. Leung, *Solid State Commun.* **125** (2003) 365
26. M. Lu, B. Chen, T, He, J. M. Tour, *Chem. Mater.* **19** (2007) 4447

27. B. K. Zhu, Z. K. Xu, *Chin. J. Appl. Chem.* **16** (1999) 68
28. W. J. Kruper, T. A. Chamberlin, M. Kochanny, *J. Org. Chem.* **5**4 (1989)
29. T. Ohtake, M. Ogasawara, K. Ito-Akita, N. Nishina, S. Ujiie, H. Ohno, T. Koto, *Chem Mater.* **12** (2000) 782
30. M. Lehmann, R. I. Gearba, M. H. J. Koch, D. A. Ivanov. *Chem. Mater.* **16** (2004) 374.